HHS Public Access

Author manuscript

Immunol Cell Biol. Author manuscript; available in PMC 2018 October 22.

Published in final edited form as:

Immunol Cell Biol. 2017 October ; 95(9): 832–842. doi:10.1038/icb.2017.55.

A Model for the Regulation of Follicular Dendritic Cells Predicts Invariant Reciprocal-Time Decay of Post-Vaccine Antibody Response

Anthony Almudevar, PhD

Department of Biostatistics and Computational Biology, University of Rochester, Rochester, NY, USA 14642, phone: (585) 275-6992, fax: (585) 273-1031

Abstract

Follicular dendritic cells (FDC) play a crucial role in the regulation of humoral immunity. They are believed to be responsible for long-term persistence of antibody, due to their role in antibody response induction and their ability to retain antigen in immunogenic form for long periods. In this article, a regulatory control model is proposed which links persistence of humoral immunity with cellular processes associated with FDCs. The argument is comprised of three elements. The first is a literature review of population-level studies of post-vaccination antibody persistence. It is found that reciprocal-time ($\propto 1/t$) decay of antibody levels is widely reported, over a range of ages, observation times, and vaccine types. The second element is a mathematical control model for cell population decay for which reciprocal-time decay is a stable attractor. Additionally, control effectors are easily identified, leading to models of homeostatic control of the reciprocal-time decay rate. The final element is a literature review of FDC functionality. This reveals a striking concordance between cell properties required by the model and those widely observed of FDCs, some of which are unique to this cell type.

The proposed model is able to unify a wide range of disparate observations of FDC function under one regulatory principle, and to characterize precisely forms of FDC regulation and dysregulation. Many infectious and immunological diseases are increasingly being linked to FDC regulation, therefore a precise understanding of the underlying mechanisms would be of significant benefit for the development of new therapies.

Introduction

Follicular dendritic cells (FDC) are found in the B-cell follicles of secondary lymph nodes. They are nonmigratory, and form a reticula network which defines a microenvironment. Their function is to capture and retain antigen in immunogenic form, and to induce antibody responses by supporting germinal centers (GC), the sites of B-cell maturation. This dual role is believed to be related to the persistence of antibody response, although the exact

Conflict of interest: The author declares no conflict of interest.

Code availability: Code used to calculate the numerical simulations shown in Figure 3 and Supplementary Figures 2-4 is available at www.urmc.rochester.edu/biostat/people/faculty/almudevar.aspx.

mechanism remains a significant open question,[1] as many infectious and immunological diseases are increasingly being linked to FDC regulation.[2,3,4] FDCs are capable of retaining unprocessed immune complexes for long periods of time, and "[f]or these characteristics, FDCs are exploited by pathogens, such as prion proteins and HIV, to persist undisturbed into the host".[3]

We present a novel mathematical control model which links regulation of antigen retention by FDCs to the reciprocal-time decay of post-vaccination antibody concentrations which is consistently reported in the literature. The model defines generalized interactions among FDCs, B-cells, and antigen-transport pathways. Balance conditions defining the steady state flow of antigen through an FDC population are defined. It is shown that under these conditions, any form of controlled FDC decay which maintains constant levels of retained antigen must result in invariant reciprocal-time decay of that FDC population, and therefore of observable antibody levels. Several classes of biologically admissible control laws are shown mathematically to maintain this steady state using a form homeostatic control. Numerical simulations demonstrate considerable robustness to various forms of perturbation.

The proposed model is supported empirically by a compendium of experimental observations compiled from two distinct literature reviews, and is able to unify disparate observations at both the population and cellular levels. Many of these observations would otherwise have no intuitive connection. A first principles model for FDC regulation is based on the following three components:

1. Reciprocal-time antibody decay. Humoral antibody persistence is a crucial outcome for vaccine development, and longitudinal antibody level measurements are regularly reported in the literature. Antibody levels are frequently observed to decay proportionally to t^k, $k < 0$, where t is the time since vaccination, referred to as power-law decay (PLD). In addition, k is consistently estimated to be close to -1 over a widely varying range of ages, observation time windows and vaccine types.

If there does exist an invariant reciprocal-time antibody decay mode ($k = -1$) this could be highly informative of regulatory processes. We offer two conjectures:

> **Conjecture 1**: Under PLD, post-vaccination antibody half-life increases with the time elapsed since the vaccine. This suggests that control of antibody decay is non-autonomous, requiring a higher degree of regulatory organization than would be possible based on time invariant decay and reaction rates.
>
> **Conjecture 2**: The invariance of reciprocal-time decay suggests a control mechanism possessing this rate of decay as a stable attractor.

2. Homeostatic control of reciprocal-time decay. A simple cellular decay model satisfies Conjectures 1-2. Suppose C_t is the concentration of a cell population $\mathcal{F}$ at time $t \geq 0$. Each cell ingests some resource at rate $\mu > 0$, and must do so to remain active. Some process regulates deactivation of cells. Deactivated cells release previously ingested resource. At time t each active cell contains ingested resource of quantity μt (assuming each is 'empty' at time $t = 0$), therefore the total resource in $\mathcal{F}$ is $F_t = \mu t C_t$. Then, if *any* regulatory process

maintains equal rates of resource flow into and out of $\mathcal{T}$, F_t will in turn maintain some constant level F_∞, resulting in reciprocal-time decay $C_t = F_\infty/\mu t$. Thus, invariant reciprocal-time decay is a consequence of steady state resource flow through the cell population, which would in turn form a target for homeostatic control. If antibody levels are maintained in proportion to C_t, then this would be observable at the population level. It is interesting to note that a very simple way of achieving this is to ensure that resource released by deactivated cells is recycled for future ingestion by the remaining active cells.

3. Follicular dendritic cells as control effectors. FDCs are reported to ingest, retain and release antigen in an immunogenic form for long periods. This ability is unique to FDCs.[1] Their continued activation is reported to depend on continual interaction with B-cells, which are also involved in antigen transport.[5] Deactivated FDCs have been observed to release ingested antigen, which remains immunogenic.[6] In addition, FDCs induce antibody production by their support of GCs.[2]

It will be shown that there is a remarkable concordance between the required cell functionality for the model cell population $\mathcal{T}$ and the known functionality of FDCs, with antigen playing the role of resource. It is interesting to note that, in addition to questions of antigen retention, the exact role played by FDCs in antibody induction remains an open question. Much of the literature describes the FDC as an antigen-presenting cell, therefore providing specific immune induction. However, alternative hypotheses describe FDC support of GCs as necessary but nonspecific, and multiple forms of GC support are described in the literature.[7,8] The relevance of the proposed model does not depend on this question. Under it, the role played by FDCs in antibody persistence is essentially that of a clock, in addition to its other functions.

Results

Models for population level antibody decay

Immune protection following vaccination is observable as the induction and maintenance of sufficiently high antibody levels over time for nearly all vaccines in use for humans. One advantage of post-vaccination follow-up studies is that antibody concentration measurements are synchronized to a common immune response starting time. Antibody half-life is commonly observed to increase in time over any scale,[9] contrasting with exponential decay resulting from spontaneous immune response cell deactivation and/or apoptosis. It seems possible, therefore, that post-vaccination antibody kinetics can be informative of specific forms of immune regulation, given that “[t]he nature of the vaccine exerts a direct influence on the type of immune effectors that are predominantly elicited and mediate protective efficacy”.[10]

Antibody concentration C_t subject to PLD can be modeled by

$$\frac{C_t}{(t-\theta)^k} = R, t > \theta, \quad (1)$$

where R is constant and θ is a time origin. A common practice is to plot concentrations against time using double-logarithmic scales, linearity being evidence of PLD (but see ref. 11). This property is not time-location invariant, so the correct identification of θ is important. However, for any θ Equation (1) approaches PLD in the limit.

Nonzero decay limits $\nu > 0$ are also proposed in the literature,[12,13] explained by competition among plasma cells for "safety niches" in bone marrow. This models antibody sources with negligible decay, which may be aggregated with PLD as

$$\frac{C_t - \nu}{(t-\theta)^k} = R, t > \theta . \quad (2)$$

We refer to (2) as the *offset power-law decay* (OPLD) model, with constraint $k = -1$ defining the *offset reciprocal-time decay* (ORTD) model. In addition, model (2) with constraints $k = -1$, $\nu = 0$ defines the *reciprocal-time decay* (RTD) model.

It has been noted by various authors that power-law decay, examples of which are reported in many fields, may have many causes, apart from a specific dynamic law, ranging from aggregation of heterogeneous processes to measurement distortion (see ref. 14 for an excellent discussion). In fact, the PLD model has been conjectured to arise as a stochastic mixture of heterogeneous exponential decay processes in the context of post-vaccine antibody kinetics,[12] yielding a model of the form

$$\log C_t = k_f - a_f \log (c_f + t), \quad (3)$$

termed the *conventional power-law decay* (CPLD) model. Long term persistence is modeled as a distinct mixture component with an essentially zero decay rate[12]

$$\log C_t = k_f + \log ((1-\pi_f)(c_f + t)^{-a_f} + \pi_f), \quad (4)$$

termed the *modified power-law decay* (MPLD) model, which reduces to (3) for $\pi_f = 0$.

Equivalence of power-law and aggregation dynamics—Note that the OPLD and MPLD models are equivalent, mapped through the reparametrization $\pi_f = \nu/(\nu + R)$, $k_f = \log(\nu + R)$, $c_f = -\theta$, $a_f = -k$. Similarly, PLD and CPLD are equivalent, using the same transformation with $\nu = \pi_f = 0$. Therefore, from a statistical point of view there is nothing to distinguish power-law and aggregation dynamics. We assume all models require definition of a decay time origin $\theta = -c_f$. Otherwise, we are left with four models distinguished by two factors. Therefore, in the context of model identification, OPLD (= MPLD) is the fully specified model, with nested submodels RTD, PLD (= CPLD) and ORTD. See Table 1 for a summary of the models.

Review of post-vaccination antibody kinetics studies

In the next two subsections we review reports of antibody decay rates from population-level post-vaccination studies. The first review includes reports in which PLD was explicitly assumed, and which also provided estimates k of the decay rate. In general, the validity of the PLD assumption was assessed using double-logarthmic plotting. The asymptote was in each case taken to be $\nu = 0$.

The second review includes studies in which geometric mean titers (GMT) of humoral antibody concentrations at fixed post-vaccination time points are tabulated. The assumptions here are more varied. In general, a wider range of models were considered, and included nonzero asymptotes $\nu \geq 0$. The studies used are listed in Table 2.

Review 1 - Empirical observation of reciprocal-time decay

The first review considers the PLD model only. Of note is that reported decay rates are consistently near $k = -1$. In one study hepatitis-B vaccine-induced antibody concentrations were measured over a period of 82 months after vaccination on 35 subects.[15] Peak concentration was reached after one month, following which PLD was consistently observed with estimated decay rate $\hat{k} = -0.9$.

Antibody decay was observed for 3085 subjects following a hepatitis-B vaccine over a 10 year period.[16] Following peak antibody concentration at 68 days, PLD with estimated decay rate $\hat{k} = -0.97$ was reported.

A *haemophilus influenzae* type b (Hib) conjugate vaccine booster dose was administered to 386 children (6 months to 4 years) following a schedule of primary doses.[17] Pre-booster (post-booster) PLD rates of $\hat{k} = -1.25$ ($\hat{k} = -0.92$) were reported.

A combination meningococcal serogroup C and Hib conjugate vaccine was adminstered to 280 healthy children aged 12-15 months[18] (data for this analysis was pooled with the study reported in ref. 17). Vaccine regimens varied, but a booster was administered following a primary dose schedule. For serogroup C-specific IgG PLD rates of $\hat{k} = -0.86, -0.95$, pre- and post-boost, were reported. The Hib (PRP-specific) IgG PLD rate $\hat{k} = -1.08, -1.00$, pre- and post-boost, were reported. Meningococcal serogroup C serum bactericidal antibody (SBA) was also assayed, and found to decay somewhat more quickly, with PLD rates $\hat{k} = -1.55, -1.60$ pre- and post-boost. The more rapid decay of the SBA was noted by the authors, offering the possibility that this is related to a disproportional representation of IgM antibodies in that form of titre.

In ref. 19 two population-based cross-sectional surveys of diphtheria antitoxin IgG concentration were analysed (collected in years 1995/1996 and 2006/2007). Analysis was limited to individuals receiving a final dose of diptheria vaccine between 8 to 9 years of age, and who were of ages 10 to 34 years (1995/1996) or 10 to 39 years (2006/2007). PLD rates of $\hat{k} = -1.20, -1.19$ were reported for the respective surveys. It should be noted that the use of natural age instead of time since vaccine renders the comparison inexact, but given the long observation window this would not lead to large differences.

Review 2 - Comparison of alternative decay models

The second review considers nonzero asymptotes $\nu \geq 0$. All four models of Table 1 are considered. We use least-squares (LS) estimates for model parameters based on log-transformed GMTs reported in the original publications. In each case, marginal 95% confidence intervals (CI) were also reported. To estimate parameters for the OPLD model the LS solutions for constrained k were calculated, then k varied. Subject level data was not used, which limits the use of formal statistical procedures or model selection methods.

Thus, it is important to note that the OPLD model is in this context the full model, the remaining models being formal reductions. This means that the error sum of squares SSE used as the fitting criterion is necessarily smallest for OPLD in every case. Therefore, absent further distributional assumptions, SSE cannot be used directly for model selection.

However, a reasonable judgement on goodness-of-fit can still be made. This would require, at a minimum, that a model's fitted values are within each CI. However, we found that in many cases the fitted values deviated very little from the reported GMTs themselves, far exceeding in stringency the criterion of CI coverage. Therefore, a positive goodness-of-fit judgement can be confidently made. In addition, in some cases alternative models yielded nearly identical fitted values, in which case any parsimony criterion would favor the simpler model.

To summarize, the objective is to identify the simplest model, if any, which successfully fits all data sets.

We note that in two cases[12] model parameters estimated in the original publication were used, as will be discussed.

HPV-16 vaccine data[12]—In ref. 12 the PLD/CPLD and OPLD/MPLD models were applied to antibody levels following HPV-16 vaccination over a 48 month study period (day 1 and months 7, 12, 18, 24, 30, 36, 42, and 48). Subjects were identified as either HPV-16 naive or HPV-16 seropositive. The models were fit from the full data using mixed effects models. Refering to the CPLD/MPLD parametrizations, the authors state that parameter c_f " … is an arbitrary small constant (often set to zero)". The fitted values for each model were reported only for the HPV-16 naive group (Supplementary Table 1), and in addition, the values of c_f were not reported.[12] They are estimated here as LS solutions, with the remaining parameters fixed at the reported values (Supplementary Table 1). Thus, where possible, we use in our analysis parameter estimates reported in the original publication.

Figure 1 shows fits for the PLD, OPLD, ORTD and RTD models. GMTs with 95% confidence limits are superimposed. For both groups, both the ORTD and OPLD models yield fits closely matching the GMTs (consistently within 95% CIs). The PLD model fails for the naive group, and the RTD model fails for both. Since both the ORTD and OPLD models yield fits compatible with the reported GMTs, this example suggests that additional parameter k in the OPLD is not needed.

Hepatitis A vaccine data[20]; Acellular pertussis (ACP) vaccine data[21]—In a vaccine trial of 110 healthy adults (hepatitis A virus seronegative) were vaccinated with an inactivated hepatitis A vaccine according to the schedule 0-1-2-12 months.[20] Subjects were randomized into 3 groups of varying vaccine dose (180, 360, 720 ELISA units per dose). GMTs and 95% CIs are reported for 13, 18, 24, 36, 84 months after vaccine (Table 1 [20]).

In an acellular pertussis (ACP) vaccine efficacy trial, IgG and IgA antibodies to pertussis toxin (PT), filamentous hemagglutinin (FHA), pertactin (PRN), and fimbriae 2/3 (FIM) were collected from 101 single-dose ACP vaccine recipients and 99 control subjects at 1, 6, 12 and 18 months after vaccination.[21] GMTs and 95% CIs are reported (Tables 1-2 [21]).

For both studies, the LS estimates of the PLD, OPLD, ORTD and RTD models were calculated. Figure 1 shows each fit (parameters are given in Supplementary Tables 2-3). In each case, the PLD, OPLD and ORTD fits were very close for all models, and well within reported 95% CIs. (The FIM GMTs did not differ significantly between vaccine and control groups.[21]) The SSE for the RTD fits were generally much larger, and the fits deviated noticeably from the alternative models, especially near the points of greatest curvature. Nonetheless, the RTD fits still remained within the reported 95% CIs (Figure 1).

Identifiability of decay models—Figure 2 plots the OPLD parameters for varying k for the HPV-16 naive subjects of ref. 12. The SSE attained for the reported OPLD/MPLD model was 0.00623[12] (Figure 2, top left). We found that $k = -2.183$ yielded the minimum SSE = 0.00184, compared to the reported value $k = -3.56$ (Supplementary Table 1).[12] Figure 2 identifies parameter regions of fits for which SSE ≤ 0.00623 (Supplementary Table 4), which are therefore at least as plausible as the OPLD/MPLD model reported in ref. 12. Yet this set contains considerable variation of parameter values. The decay rate itself varies within $k \in [-3.72, -1.38]$, and rate $k = -1$ has already been shown to yield a model compatible with the reported GMTs. A similar effect can be seen for the HPV-16 seropositive group (Supplementary Figure 1).

Additionally, ν represents the limiting antibody concentration, with values $\nu \in [105.67, 130.39]$ associated with models for which SSE ≤ 0.00623. Furthermore $\nu = 86.2$ for the ORTD model. One goal of identifying antibody kinetics is to enable comparison to minimum protective antibody levels (MPL). This value has not yet been determined for commercialized HPV vaccines.[22,23] Conjectured values of 20 and 100 mMU/mL were used in ref. 12 to predict long-term protection. This upper bound is well within the range of plausible values of ν among the various models considered. In addition, there is a tendency in the OPLD/MPLD model for the estimate of ν to be close to the minimum reported GMT (Supplementary Tables 1-3). Therefore, the comparison of MPLs to vaccine kinetics cannot be resolved within this parametric framework.

Accurate estimates of curvature require a suitably higher density of time points where curvature is greatest. However, what is most needed is a scientifically validated model for which parameters can be confidently interpreted. Thus, while it is important to note that reciprocal-time decay (with or without limit ν) was able to explain every example of

antibody kinetics examined here, the next crucial step is to propose a plausible first-principles model which predicts reciprocal-time decay. We consider this problem next.

Function of FDCs

A number of review articles describe FDC origin, structure and functionality.[24,25,2,1,4] The following properties are consistently reported.

(A1) FDC architecture forms a microenvironment within secondary lymph nodes.

(A2) FDCs are capable of ingesting and storing antigen for long periods of time. Ingested antigen is not degraded, and remains immunogenic.

(A3) FDCs require persistent signaling to remain active.

(A4) When an FDC is inactivated, it can no longer ingest or retain antigen.

(A5) FDCs stimulate antibody production via support of GCs.

Regarding (**A1**), FDCs are nonmigratory, and collectively create a "sponge-like" network of reticula in which antigen is retained, defining a microenvironment in which they interact with B-cells in several ways.[24]

Property (**A2**) describes the long-term retention of antigen in lymph tissue cells in a functional state, which has been confirmed by earlier experimental observations.[26,27,28] Antigen, in the form of immune complexes (IC) of antigen-antibody pairs, can be acquired by interaction with naive antigen transporting B-cells. The ICs are stored by FDCs as membrane-coated bodies known as iccosomes. FDCs are capable of returning ingested antigen to the cell surface. In fact, single antigen particles can be observed to cycle multiple times between cell surface and cell interior.[29] The ability of FDCs to retain intact antigen for extended periods is unique.[1]

Regarding properties (**A3**)-(**A4**), maintenance of FDC functionality requires continual lymphotoxin α/β (LT) signaling (with tumour necrosis factor (TNF) playing a similar role).[5] Inhibition of LT signaling not only prevents FDC trapping of ICs, but eliminates previously trapped ICs. The authors of ref. 5 write that "[a] surprising observation is that the maintenance of pre-existing FDCs in a differentiated state requires continual interaction with B lymphocytes expressing LTα/β". FDCs produce the B-cell attractant CXCL13. This mechanism is part of a positive feedback loop.[30]

Regarding (**A5**), GCs are recognized as the site of the induction of B-cell memory, and the close association of GCs and FDCs is widely reported. The ratio of FDC antigen retaining reticula and GCs was reported to be 1:1 in mouse lymph tissue.[24] That active GCs require FDC support in the normal immune response is widely accepted. However, it has been proposed[7] that antigen-presentation by FDCs is not required for GC function, and the question of whether GC support is specific or non-specific is still being considered.[1,4,8] Nonetheless, our model does not depend on the exact form of GC/FDC interaction. We only argue that under certain steady state conditions FDC populations decay by reciprocal-time, and so would any FDC-dependent antibody production.

Decay of FDC concentration is concurrent with antigen retention—In ref. 24 a time series of concentrations of injected radio-labeled antigen within mouse lymph tissue was reported. According to the authors "… it is … significant that nearly half of the follicles that had an antigen-retaining reticulum on [day] 3 lost it by [day] 5. It appears that the FDC in some follicles release all the localized antigen by [day] 3, apparently by iccosome release, while the antigen persists in other follicles for long-term retention."

Control model for FDC decay

We next develop the mathematical model for homeostatic control of reciprocal-time decay introduced above (some details of the mathematical argument are given in the Supplementary Material). We first verify the equivalence of antibody and FDC kinetics. We consider a kinetic model in which antibody $A(t)$ decays at rate $\mu_a > 0$, and in which antibody production is stimulated by cells $B(t)$ at rate $\lambda_b > 0$ for a total antibody rate[13]

$$\frac{dA}{dt} = -\mu_a A(t) + \lambda_b B(t). \quad (5)$$

If the decay of $B(t)$ is slower than spontaneous antibody decay, then it is this decay rate which will be observed. Under property (**A5**) decay of FDC-induced antibody would then be proportional to FDC population decay. This is stated in Theorem 1. The essential condition on $B(t)$ is given in terms of its decay rate. This need not be constant. All that is required is that the decay rate of $B(t)$ remain less than, and bounded away from, μ_a. In this case $A(t)$ and $B(t)$ have the same asymptotic decay rate.

Theorem 1. In Equation (5), suppose $B(t)$ possesses derivative $B'(t)$, and there exist constants $a_L \leq a_U$ for which

$$-\mu_a < a_L = \liminf_{t\to\infty} \frac{B'(t)}{B(t)} \leq \limsup_{t\to\infty} \frac{B'(t)}{B(t)} = a_U. \quad (6)$$

Then

$$\frac{\lambda_b}{\mu_a + a_U} \leq \liminf_{t\to\infty} \frac{A(t)}{B(t)} \leq \limsup_{t\to\infty} \frac{A(t)}{B(t)} \leq \frac{\lambda_b}{\mu_a + a_L}. \quad (7)$$

Proof. See Supplement S.1 for proof.

Model definition—Suppose there exists a population of activated FDCs, the initial size being a positive real number $N \in \mathbb{R}$ The model system $\mathscr{S}$ is partitioned into a reservoir $\mathfrak{R}$ and an FDC population $\mathfrak{F}$. Flow through $\mathscr{S}$ is given by:

External antigen source $\rightarrow \mathscr{R} \rightarrow \mathscr{F} \rightarrow$ Antigen clearance .

The system $\mathscr{S}$ can be taken to be the microenvironment created by the FDC population (property (**A1**)). Antigen transport pathways exist in $\mathscr{R}$, while antigen retained in FDCs exists in $\mathscr{F}$.

Let C_t, F_t be the population size of still active FDCs and the total amount of antigen in $\mathscr{F}$ at time $t \in [0, \infty)$, respectively. We take $C_t \in [0, N]$, $F_t \in [0, \infty)$ to be real valued, with initial values $C_0 = N$, $F_0 = 0$. We also need to define the amount of antigen $E_t \in [0, \infty)$ contained in $\mathscr{R}$. This is the antigen available for FDC ingestion.

Define the following rules:

(**B1**) As long as a unit FDC remains active it ingests antigen at a rate of μ per unit time.

(**B2**) A unit FDC may be deactivated at any time, at which point its total ingested antigen is released.

(**B3**) No FDC can be created or reactivated.

System steady state—We next characterize the steady state mathematically, and describe the implications for FDC kinetics. Under rules (**B1**)-(**B3**) the balance equation

$$F_t = \mu t C_t, t \geq 0 \quad (8)$$

must hold. Differentiating (8) gives

$$\frac{dF_t}{dt} = \mu\left[C_t + t\frac{dC_t}{dt}\right]. \quad (9)$$

The terms of Equation (9) are easily interpretable. Antigen is ingested at a rate of μ per unit cell, giving the term μC_t. At time t a unit FDC has ingested μt units of resource, therefore a decay rate of $dC_t/dt < 0$ forces release of antigen from $\mathscr{F}$ at the rate $-\mu t dC_t/dt$.

Thus, the system steady state $dF_t/dt = 0$ is characterized by both constant antigen retention $F_t = F_\infty$ and reciprocal-time decay of the FDC population $C_t = F_\infty/\mu t$.

Negative feedback mechanism for homeostatic control—We now show how reciprocal-time decay may be characterized as an attractor. This describes any stable mode of behavior towards which a systems tends from a large set of initial states. In fact, the model possesses a natural control effector in the form of a parameter which may be regulated to correct deviations from the steady state. Define the double-logarithmic derivative

$$k_t = \frac{d \log C_t}{d \log t} = \frac{C_t^{-1} dC_t}{t^{-1} dt}.$$

The solution to $k_t \equiv k$ yields the relation

$$\frac{C_t}{C_s} = \left(\frac{t}{s}\right)^k, s, t > 0. \quad (10)$$

We may then express (9) as

$$\frac{dF_t}{dt} = \mu \cdot C_t[1 + k_t], \quad (11)$$

from which the control effector emerges. Maintaining $k_t \equiv -1$ forces $dF_t/dt = 0$, and $k_t > -1$ or $k_t < -1$ forces increase or decrease in F_t, respectively. Thus, feedback control of k_t, which determines the decay rate of C_t, provides a negative feedback mechanism for homeostatic maintenance of the system steady state. Interestingly, the steady state forces continual decay of C_t.

Forms of control law—The problem is then to propose a biologically admissible control law for k_t with the system steady state as an attractor. It would be reasonable to assume that control is effected at the individual cell level, taking the form

$$\frac{dC_t}{dt} = -\bar{\lambda}(F_t, C_t, t)C_t \quad (12)$$

for some *unit cell decay* control functon $\bar{\lambda} \geq 0$. We can substitute the balance equation (8) into (12) to obtain a first-order ordinary differential equation (ODE):

$$\frac{dC_t}{dt} = -\bar{\lambda}(\mu t C_t, C_t, t)C_t. \quad (13)$$

In this form, $\bar{\lambda}$ could be interpreted as a stochastic FDC failure rate following some sequence of signaling or interaction events. Note that the instantaneous population half-life is $t_{1/2} = \log(2)/\bar{\lambda}$, so if $\bar{\lambda}$ is bounded above we must have $C_t > 0$, $t > 0$.

Exponential decay cannot yield homeostatic control—Spontaneous population decay with constant half-life defines exponential decay. This cannot direct the system to its

steady state. To see this, suppose $\mathfrak{R}$ always contains sufficient antigen for FDC ingestion, and the unit cell decay rate is constant at $\bar{\lambda}(F_t, C_t, t) \equiv \rho > 0$, resulting in exponential population decay. The solution to (12) is $C_t = C_0 \exp(-\rho t)$, in which case $F_t = \mu t C_0 \exp(-\rho t)$. This function possesses a global maximum at $t = 1/\rho$. Therefore, F_t increases to peak level $F_{max} = (\mu/\rho) C_0 \exp(-1)$ then converges to zero.

Steady state antigen flow through FDC population $\mathfrak{F}$—We next consider what form of control is required for homeostasis. Under system steady state we have

$$\frac{dC_t}{dt} = -\frac{C_t}{t}, t > 0,$$

so that

$$\bar{\lambda}(F_t, C_t, t) = t^{-1}. \quad (14)$$

However, what is needed is a control function $\bar{\lambda}$ in the form of a time-homogenous closed-loop control law which yields robust maintenance of the steady state through simple negative feedback mechanisms, and which is compatible with known FDC functionality.

Control for which unit cell decay is proportional to FDC concentration—One possibility is that FDC deactivation is upregulated in proportion to population concentration. Under the balance conditions of (8), (14) is equivalent to

$$\bar{\lambda}(F_t, C_t, t) = \frac{\mu C_t}{F_t}, \quad (15)$$

which approaches in the limit

$$\bar{\lambda}(F_t, C_t, t) = \frac{\mu C_t}{F_\infty}. \quad (16)$$

We show, conversely, that a control law of the form (16) possesses the system steady state as an attractor. Suppose we are given for some $a > 0$ control function

$$\bar{\lambda}(F_t, C_t, t) = aC_t. \quad (17)$$

This yields ODE

$$\frac{dC_t}{dt} = -aC_t^2.$$

The solution

$$C_t = \frac{1}{at + 1/C_0}, t \geq 0, \quad (18)$$

is easily verified by direct substitution. It is important to note that (18) differs from (10) in several important respects. The relationship (10) is defined on logarithmic time while (18) is defined for additive time, with reciprocal-time decay approached as a limit. Thus, for (10) if $s > 0$ is an initial time, we have $C_t = C_s(s/t)$, and C_t is uniformly proportional to initial value C_s. In contrast, in (18) C_t is not uniformly proportional to C_0, and the dependence on C_0 vanishes in the limit. Given the balance conditions of (8) this means the steady state retained-antigen level F_∞ is

$$F_\infty = \lim_{t \to \infty} F_t = \lim_{t \to \infty} \mu t C_t = \mu a^{-1},$$

which depends on control parameter a, ingestion rate μ, but not initial cell concentration C_0.

It will be useful to generalize the control function (17) in the following way.

Theorem 2. Suppose we are given some function $a : (0, C_0) \mapsto (0, \infty)$, possessing derivative a', such that the control function for ODE (12) is given by

$$\bar{\lambda}(F_t, C_t, t) = a(C_t)C_t, \quad (19)$$

where $\lim_{c \downarrow 0} a(c) = \bar{a} \in (0, \infty)$ and $|a'(c)| < \infty$ for all $c \in (0, K_C)$ for some positive constant $K_C \leq C_0$. Then

$$\lim_{t \to \infty} tC_t = \bar{a}^{-1}. \quad (20)$$

Proof. See Supplement S.2 for proof.

Balance equations for steady state antigen flow through system $\mathscr{S}$—We next expand the model to allow a role for antigen transport and availability in FDC regulation. Suppose we have initial reservoir level $E_0 = R > 0$. Let A_t be the total amount of additional

antigen entering $\mathcal{R}$ by time t. Then let B_t be the total antigen released by deactivated FDCs by time t. We must have

$$\frac{dB_t}{dt} = -\mu t \frac{dC_t}{dt}. \quad (21)$$

Assuming B_t is lost to the system, the balance equation may be expanded to

$$\begin{gathered} F_t = \mu t C_t, \\ R + \Delta_t = E_t + F_t, t \geq 0 \text{ where } \Delta_t = A_t - B_t. \end{gathered} \quad (22)$$

The control functon $\bar{\lambda}$ may depend on any of the quantities in (22), assuming they satisfy the balance conditions, and so the system remains governed by the ODE:

$$\frac{dC_t}{dt} = -\bar{\lambda}(A_t, B_t, C_t, E_t, F_t, t) C_t. \quad (23)$$

If the net flow of antigen through $\mathcal{S}$ is zero, that is, the additional balance condition $\Delta_t = 0$ holds, then convergence to the steady state can be expressed as:

$$\lim_{t \to \infty} E_t = E_\infty < R. \quad (24)$$

In other words, under the system steady state $\mathcal{R}$ is indefinitely depleted in part or in full. In this case $F_\infty = R - E_\infty$, forcing invariant reciprocal-time decay $C_t = (R - E_\infty)/\mu t$.

Control based on allocation of available antigen—As an alternative to control based on FDC population concentration, suppose FDC deactivation is upregulated by antigen scarcity. An average antigen concentration of E_t/C_t is available to each FDC. Suppose the FDC remains active as long as it ingests antigen (mediated via known signaling processes), and has a maximum ingestion rate capacity of μ. To develop a simple stochastic failure rate model, suppose antigen is made available to an FDC as a Poisson process with arrival rate γ^* and FDC is deactivated if it does not ingest antigen within a time period κ. The failure rate is therefore the rate at which interarrival times exceeding κ occur. Then, if the arrival process is the aggregation of individual antigen arrival processes of rate γ we would expect $\gamma^* = \gamma E_t/C_t$, leading to failure rate

$$\bar{\lambda}(C_t, E_t) = \begin{cases} \gamma E_t / C_t \exp(-\gamma\kappa E_t / C_t) & ; \ E_t > 0 \\ \infty & ; \ E_t = 0 \end{cases}. \quad (25)$$

See Supplement S.3 for details. To remain active, the aggregate antigen arrival rate γ^* for an individual FDC must be larger than μ. Under these conditions, the neighborhood of an FDC is essentially saturated with available antigen, and therefore able to maintain the maximum ingestion rate μ. As antigen is depleted the quantity E_t/Ct decreases, forcing γ^* to approach μ, making an ingestion failure event increasingly likely Thus, this failure model predicts property (**B1**). Convergence to reciprocal-time decay when net antigen flow is zero is verified in the following theorem:

Theorem 3. Suppose the control function $\bar{\lambda}$ of ODE (23) is given by Equation (25). Suppose $\Delta_t \equiv 0$ in balance equations (22). Then there exists a constant t^*, dependent only on parameters (μ, γ, κ) for which the following statements hold:

i. For any initial state $(t, C_t) = (t_0, C_{t_0})$ for which $t_0 > t^*$ there exists a positive constant r^* such that for all large enough R^* we have:

$$0 < C_t < \frac{R^*}{\mu t + r^*},$$

and therefore $E_t/C_t > r^*$, $t \geq t_0$, where $R^* = E_0$ is taken to be the initial reservoir quantity.

ii. Given the initial conditions of (i), if $E_0 = R^*$ then $\lim_{t\to\infty} \mu t C_t = R^*$.

Proof. See Supplement S.4 for proof.

Thus, under the conditions of Theorem 3, C_t possesses reciprocal-time decay in the limit, and steady state antigen retention $\lim_{t\to\infty} F_t = R$, with complete reservoir depletion $\lim_{t\to\infty} E_t = 0$. The steady state retention level F_∞ therefore depends on R but not on control or model parameters (μ, γ, κ).

Numerical simulations

We present a number of computer simulations of model (9). Balance equations (22) are assumed to hold with $\Delta_t = 0$. We take time interval $t \in [0, 1000]$, with $C_0 = 10^3$. We vary the initial resource by setting $R/C_0 = 25000, 5000, 1000$. The antigen ingestion rate is set to $\mu = 10^3$. We use the antigen allocation control model with failure rate $\hat{\lambda}$ given by Equation (25) (see also Supplement S.3). To determine a value for γ, consider the case $R/C_0 = 1000$. This gives an antigen arrival rate per FDC at $t = 0$ of $\gamma E_0/C_0 = \gamma R/C_0 = \gamma 1000$. Equating this to μ gives $\gamma = 1$. Given ingestion rate μ it would be reasonable to set κ to be some factor of μ^{-1}, so we set $\kappa = \mu^{-1} = 1/1000$. The model was discretized by time intervals $\Delta t = 10^{-4}$.

Figure 3 shows model pathways for varying initial resource $R/C_0 = 25000, 5000, 1000$ (columns 1-3). In row 1 plots of C_t and E_t are shown with a vertical log scale. Row 2 shows

C_t and E_t on a log-log scale. Grid lines parallel to t^{-1} are superimposed. For display E_0, C_0 are both normalized to equal 100% in rows 1-2. Additionally, in Supplementary Figure 2 row 1 gives the double logarithmic decay rate k_t as a function of time, and row 2 gives the relative concentration of retained antigen F_t/R.

The behavior for each set of initial conditions is similar. Each example begins with a short period of decay k_t close to 0, then begins approaching $k_t = -1$ by times ranging from $t \approx 100 – 250$, as can be seen in the log-log plot and the plot of k_t (row 2 of Figure 3, row 1 of Supplementary Figure 2). F_t quickly reaches its predicted steady state level R (Supplementary Figure 2, row 2).

Robustness to random perturbations—Supplementary Figure 3 is based on the same model used for Figure 3($R/C_0 = 25000$) but with various forms of stochastic noise introduced (columns 1-3). For the "random resource spikes" model the reservoir $\mathcal{R}$ was supplemented by bulk arrivals of 500 antigen units according to a Poisson process of rate 0.04. For the remaining models multiplicative noise was incorporated by multiplying dC_t/dt by a log-normal random variable at each computation point (the exponentiated normal random variates had mean $\mu = 0$ and standard deviations $\sigma = 0.1, 1$).

In each case the models exhibit the same limiting behavior seen in Figure 3, despite persistent random perturbations. For the random resource spikes model the assumption of constant system resource R is violated, but without apparent effect on the approach to the predicted system steady state (Supplementary Figure 3, column 1).

For the multiplicative noise model with $\sigma = 0.1$ (Supplementary Figure 3, column 2), the behavior differs little from the corresponding noiseless model (Figure 3, column 1). What is of some interest is the stable fluctuation of k_t about the steady state value $k = -1$, suggesting an efficient negative feedback control able to maintain reciprocal-time decay. Setting $\sigma = 1$ results in considerably more noise (Supplementary Figure 3, column 3). The decay rate k_t no longer fluctuates about $k = -1$ in a stable manner, but instead subjects the system to frequent and extremely large decay rates. In this case, fluctuation of E_t is more evident (rows 1,2). Despite this, the system steady state is maintained.

Deviation from balanced antigen flow through system $\mathcal{S}$—We next allow Δ_t in balance equation (22) to vary. Otherwise the model of Figure 3 ($R/C_0 = 25000$) is used. We consider three deviation models:

1. **Autoregressive Deviation:** $\Delta_t = (R - F_t)Z_t$, where Z_t is an autoregressive Gaussian process with stationary standard deviation $\sigma_z = 1/8$ and correlation $\rho \approx 0.905$ per unit time.
2. **Sine Wave Deviation:** $\Delta_t = (R - F_t) \sin(2\pi t/100)/2$.
3. **Finite Resource Leak:** $d\Delta_t/dt = ct^{-2}$, where c is chosen so that $\Delta_{1000} = -R/10$.

For models 1 and 2, deviation is scaled by $R — F_t$, representing the reservoir contents for deviation $\Delta_t = 0$. For model 3, antigen leaks at a rate proportional to t^{-2}, the cumulative amount being $R/10$. Graphical summaries are given in Supplementary Figure 4.

As can be seen for deviation models 1 and 2, fluctuation of the total antigen content of system $\mathscr{S}$ forces fluctuation of the decay rate k_t about −1. However, in each case the limiting behavior of C_t, E_t and F_t is little changed, especially the reciprocal-time decay of C_t (compare to Figure 3, column 1). The same conclusion can be reached of deviation model 3, except that the antigen leak appears to have a small depressing effect on F_t. In each case, homeostatic maintenance of the system steady state is clearly evident.

Discussion

We next offer Remarks (1)-(6) regarding the proposed control model.

Remark 1. Similar to the antigen allocation model (25), the decay rate (16) is interpretable in terms of failure events. Suppose for each small time interval Δt there are m independent failure events, each occuring with a proportionally small probability $q\Delta t$. If failure occurs with the occurrence of at least one failure event, failure rate $\bar{\lambda}$ is given by

$$\bar{\lambda}\Delta t = 1 - (1 - q\Delta t)^m \approx mq\Delta t\,. \quad (26)$$

If the number of failure events m is proportional to C_t this would yield failure rate $\bar{\lambda} \propto C_t$. Theorem 2 would then be applied to verify that $\lim_{t\to\infty} tC_t = a^{-1}$.

In contrast, for the antigen allocation model (25) we may write, for some probability p,

$$\bar{\lambda}\Delta t \approx mp^m\Delta t = p^{m+o(m)}\Delta t \quad (27)$$

where $m \propto E_t/C_t$, the average available antigen per FDC, and $o(m)$ is negligible compared to large m.

A failure rate of the form (26) describes a series failure rate (system failure requires only 1 of m failure events to occur) while (27) describes a parallel failure rate (system failure requires all of m failure events to occur). What both failure models have in common is that the decay rate tends to be inversely related to C_t, which provides a link between cellular level processes and the control parameter k_t given in Equation (11).

Remark 2. Following Remark (1), under control function (16) the steady state level of retained antigen in $\mathscr{R}$ is $F_\infty = \mu a^{-1}$, while under control function (25) it is $F_\infty = R$. The former depends on component interaction rates, while the latter is simply the net antigen R retained by the system $\mathscr{S}$. Thus, while each control yields reciprocal-time decay, they could, in principle, be distinguished by suitable experimental perturbations.

Remark 3. We next consider the question of how the initial state is attained, particularly since property (**B3**) holds that active FDCs cannot be added to $\mathscr{T}$. This assumes that the entire process consists of two phases, the first in which the FDC population is created up to N cells, followed by a period in which deactivation predominates. However, the model

assumes $F_0 = 0$ when $E_0 = R$, that is, the FDCs contain no antigen when the decay process begins.

Suppose, to fix ideas, the N initial FDCs have been ingesting antigen for a period of time equal to τ before the decay phase begins (at $t = 0$). Then the differential balance equation (9) must be modifed to become

$$\frac{dF_t}{dt} = \mu\left[C_t + (t+\tau)\frac{dC_t}{dt}\right]. \quad (28)$$

However, it is easily verified that the steady state solution to $dF_t/dt = 0$ is $C_t \propto (t+\tau)^{-1}$, so that the original system is recovered by a simple time offset.

Remark 4. The model has so far not considered antigen lost by presentation, or some other mechanism. We have assumed that B_t consists entirely of antigen lost by FDC deactivation (21). Suppose we assume that antigen is used for presentation, and is lost to the system, at a constant rate $\eta > 0$ per cell. Then the differential balance equation (9) must be modifed to become

$$\frac{dF_t}{dt} = \mu\left[C_t + t\frac{dC_t}{dt}\right] - \eta C_t. \quad (29)$$

The steady steady state solution to $dF_t/d_t = 0$ is now $C_t \propto t^{-1+\eta/\mu}$. However, if we assume that $\eta \ll \mu$ then the deviation from reciprocal-time decay would be minimal. This would occur, for example, if any amount of antigen presented is small compared to the amount retained.

Remark 5. We next consider the question of how antigen can be retained in the FDC population indefinitely. Our model describes a decay process based on the simple balance equation $\mu t C_t = F_t$. This assumes continuous ingestion of antigen by FDCs, and a balanced flow of antigen through the system $\mathscr{S}$. However, by (21) it can be seen that under reciprocal-time decay of C_t we have $B_t \propto \log(t)$, therefore antigen must flow through $\mathscr{S}$ indefinitely. This may limit the duration of the reciprocal-time FDC decay regulation.

Another intriguing possibility is that any antigen released by deactived FDCs is simply returned to $\mathscr{R}$ to be ingested again. This would force $A_t = B_t$, and the steady state could be maintained indefinitely. This idea seems compatible with a number of observations made in the literature. The possibility of antigen exchange between FDCs was raised in ref. 31. In ref. 6 an experimental method of releasing antigen iccosomes from FDCs was reported. In the absence of active FDCs, very little specific antibody response was observed following release. When active but specific antigen negative FDCs were introduced, specific antibody response increased dramatically. When FDCs and B-cells were separated by an iccosome permeable membrane, antibody response was suppressed. In addition, multiple transport

pathways for antigen delivery to FDCs are known.[32] It is conceivable, therefore, that a specialized antigen-transport pathway could exist for the recycling of antigen in this manner.

Remark 6. Following Remark 5, it must be noted that even if a fixed amount of antigen can be retained indefinitely, by rule (**B1**) this implies an unbounded capacity of a single FDC for antigen retention. Certainly, the dendritic architecture of the FDC appears to be designed precisely for large scale antigen storage.[24] But clearly, some limit must eventually be reached, whether by depletion of antigen available for ingestion, or by saturation of the FDC itself. Therefore, FDC reciprocal-time decay regulation might be more usefully considered to be only a single phase in the production of antibodies, the duration of which is either itself regulated, or dependent on exogenous conditions. In fact, the review of post-vaccination antibody kinetics studies above suggests this possibility.

Summary

In conclusion, a mathematical model for the controlled deactivation of FDC was proposed. The system steady state is characterized by constant levels of retained antigen, and the reciprocal-time decay of the FDC population. Given the FDCs role in the stimulation of antibody production via GCs, this may explain the consistent observation of reciprocal-time decay in post-vaccination antibody concentrations. The specific properties required by FDCs by the model are in striking concordance with those consistently observed, in particular the long-term retention of antigen; the simultaneous decay of FDC populations; the associated antigen-delivery pathways; and the persistent signalling required for their continuous activation. Furthermore, it was shown that this steady state can be robustly maintained by simple biologically admissible forms of homeostatic control.

As stated in ref. 2: “[a] better understanding of FDCs should permit better regulation of antibody responses to suit the therapeutic manipulation of regulated and dysregulated immune responses.”

Supplementary Material

Refer to Web version on PubMed Central for supplementary material.

Acknowledgments

This work was supported by NIH grant 14.243092-001 and by the Rochester General Hospital Research Institute. The author is especially grateful for the support of Dr. Michael Pichichero.

References

1. Heesters BA, Myers RC, Carroll MC. Follicular dendritic cells: Dynamic antigen libraries. Nat Rev Immunol. 2014; 14:495–504. [PubMed: 24948364]
2. El Shikh ME, Pitzalis C. Follicular dendritic cells in health and disease. Front Immunol. 2012; 3:292. [PubMed: 23049531]
3. Melzi E, Caporale M, Rocchi M, Martín V, Gamino V, di Provvido A, et al. Follicular dendritic cell disruption as a novel mechanism of virus-induced immunosuppression. Proc Natl Acad Sci USA. 2016:E6238–E6247. [PubMed: 27671646]
4. Kranich J, Krautler NJ. How follicular dendritic cells shape the B-cell antigenome. Front Immunol. 2016; 7:225. [PubMed: 27446069]

5. Mackay F, Browning JL. Turning off follicular dendritic cells. Nature. 1998; 395:26–27. [PubMed: 9738494]
6. Wu J, Qin D, Burton GF, Szakal AK, Tew JG. Follicular dendritic cell-derived antigen and accessory activity in initiation of memory IgG responses in vitro. J Immunol. 1996; 157:3404–3411. [PubMed: 8871638]
7. Haberman AM, Shlomchik MJ. Reassessing the function of immune-complex retention by follicular dendritic cells. Nat Rev Immunol. 2003; 3:757–764. [PubMed: 12949499]
8. Wang X, Cho B, Suzuki K, Xu Y, Green JA, An J, et al. Follicular dendritic cells help establish follicle identity and promote B cell retention in germinal centers. J Exp Med. 2011; 208:2497–2510. [PubMed: 22042977]
9. Gajdos V, Soubeyrand B, Vidor E, Richard P, Boyer J, Sadorge C, et al. Immunogenicity and safety of combined adsorbed low-dose diphtheria, tetanus and inactivated poliovirus vaccine (REVAXIS®) versus combined diphtheria, tetanus and inactivated poliovirus vaccine (DT Polio®) given as a booster dose at 6 years of age. Hum Vaccin. 2011; 7:549–556. [PubMed: 21441781]
10. Siegrist CA. Vaccine Immunology. In: Plotkin SA, Orenstein WA, Offit PA, editorsVaccines. Elsevier Inc; Philadelphia, PA: 2008. 17–36.
11. Clauset A, Shalizi CR, Newman MEJ. Power-law distributions in empirical data. SIAM Rev. 2009; 51:661–703.
12. Fraser C, Tomassini JE, Xi L, Golm G, Watson M, Giuliano AR, et al. Modeling the long-term antibody response of a human papillomavirus (HPV) virus-like particle (VLP) type 16 prophylactic vaccine. Vaccine. 2007; 25:4324–4333. [PubMed: 17445955]
13. Andraud M, Lejeune O, Musoro JZ, Ogunjimi B, Beutels P, Hens N. Living on three time scales: The dynamics of plasma cell and antibody populations illustrated for hepatitis A virus. PLoS Comput Biol. 2012; 8:e1002418. [PubMed: 22396639]
14. Wixted JT. On common ground: Jost's (1897) law of forgetting and Ribot's (1881) law of retrograde amnesia. Psychol Rev. 2004; 111:864–879. [PubMed: 15482065]
15. Gesemann M, Scheiermann N. Quantification of hepatitis B vaccine-induced antibodies as a predictor of anti-HBs persistence. Vaccine. 1995; 13:443–447. [PubMed: 7639012]
16. Honorati M, Palareti A, Dolzani P, Busachi C, Rizzoli R, Facchini A. A mathematical model predicting anti-hepatitis B virus surface antigen (HBs) decay after vaccination against hepatitis B. Clin Exp Immunol. 1999; 116:121–126. [PubMed: 10209515]
17. Southern J, McVernon J, Gelb D, Andrews N, Morris R, Crowley-Luke A, et al. Immunogenicity of a fourth dose of Haemophilus influenzae type b (Hib) conjugate vaccine and antibody persistence in young children from the United Kingdom who were primed with acellular or whole-cell pertussis component-containing Hib combinations in infancy. Clin Vaccine Immunol. 2007; 14:1328–1333. [PubMed: 17699835]
18. Borrow R, Andrews N, Findlow H, Waight P, Southern J, Crowley-Luke A, et al. Kinetics of antibody persistence following administration of a combination meningococcal serogroup C and Haemophilus influenzae type b conjugate vaccine in healthy infants in the United Kingdom primed with a monovalent meningococcal serogroup C vaccine. Clin Vaccine Immunol. 2010; 17:154–159. [PubMed: 19906895]
19. Swart E, van Gageldonk P, de Melker H, van der Klis F, Berbers G, Mollema L. Long-term protection against diphtheria in the Netherlands after 50 years of vaccination: Results from a seroepidemiological study. PloS One. 2016; 11:e0148605. [PubMed: 26863307]
20. Wiedermann G, Kundi M, Ambrosch F, Safary A, D'Hondt E, Delem A. Inactivated hepatitis A vaccine: long-term antibody persistence. Vaccine. 1997; 15:612–615. [PubMed: 9178459]
21. Le T, Cherry JD, Chang SJ, Knoll MD, Lee ML, Barenkamp S, et al. Immune responses and antibody decay after immunization of adolescents and adults with an acellular pertussis vaccine: the APERT Study. J Infect Dis. 2004; 190:535–544. [PubMed: 15243929]
22. Longet S, Schiller JT, Bobst M, Jichlinski P, Nardelli-Haefliger D. A murine genital challenge model is a sensitive measure of protective antibodies against human papillomavirus infection. J Virol. 2011; 85:13253–13259. [PubMed: 21976653]

23. Endo F, Tabata T, Sadato D, Kawamura M, Ando N, Oboki K, et al. Development of a simple and quick immunochromatography method for detection of anti-HPV-16/-18 antibodies. PloS One. 2017; 12:e0171314. [PubMed: 28158224]

24. Tew JG, Kosco MH, Burton GF, Szakal AK. Follicular dendritic cells as accessory cells. Immunol Rev. 1990; 117:185–211. [PubMed: 2258191]

25. Liu YJ, Grouard G, de Bouteiller O, Banchereau J. Follicular dendritic cells and germinal centers. Int Rev Cytol. 1996; 166:139–179. [PubMed: 8881775]

26. Nossal G, Ada G, Austin CM. Antigens in immunity. X. Induction of immunologic tolerance to Salmonella adelaide flagellin. J Immunol. 1965; 95:665–672. [PubMed: 5841054]

27. Nossal G, Abbot A, Mitchell J. Antigens in immunity. XIV. Electron microscopic radioautographic studies of antigen capture in the lymph node medulla. J Exp Med. 1968; 127:263–276. [PubMed: 5635379]

28. Tew J, Mandel T. Prolonged antigen half-life in the lymphoid follicles of specifically immunized mice. Immunology. 1979; 37:69–76. [PubMed: 468304]

29. Heesters BA, Chatterjee P, Kim YA, Gonzalez SF, Kuligowski MP, Kirchhausen T, et al. Endocytosis and recycling of immune complexes by follicular dendritic cells enhances B cell antigen binding and activation. Immunity. 2013; 38:1164–1175. [PubMed: 23770227]

30. Ansel KM, Ngo VN, Hyman PL, Luther SA, Förster R, Sedgwick JD, et al. A chemokine-driven positive feedback loop organizes lymphoid follicles. Nature. 2000; 406:309–314. [PubMed: 10917533]

31. Jarjour M, Jorquera A, Mondor I, Wienert S, Narang P, Coles MC, et al. Fate mapping reveals origin and dynamics of lymph node follicular dendritic cells. J Exp Med. 2014; 211:1109–1122. [PubMed: 24863064]

32. Heesters BA, Carroll MC. The role of dendritic cells in s. pneumoniae transport to follicular dendritic cells. Cell Rep. 2016; 16:3130–3137. [PubMed: 27653679]

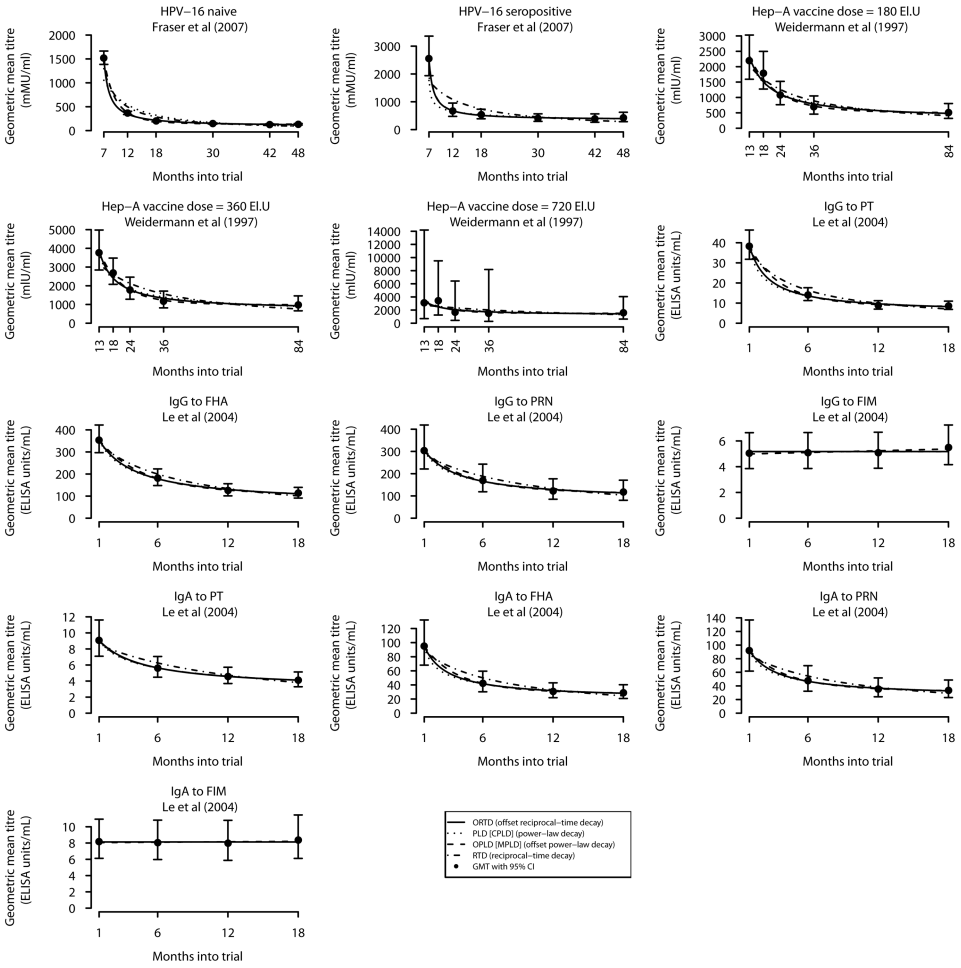

Figure 1.

Fitted curves for antibody decay models using data from ref. 12,ref. 20 and ref. 21. For the HV16 naive group of ref. 12 (row 1, column 1) plot show the fits for the PLD/CPLD and OPLD/MPLD models using the parameters reported in ref. 12, using the LS estimate of c_f. Otherwise, fits were calculated using the LS method.

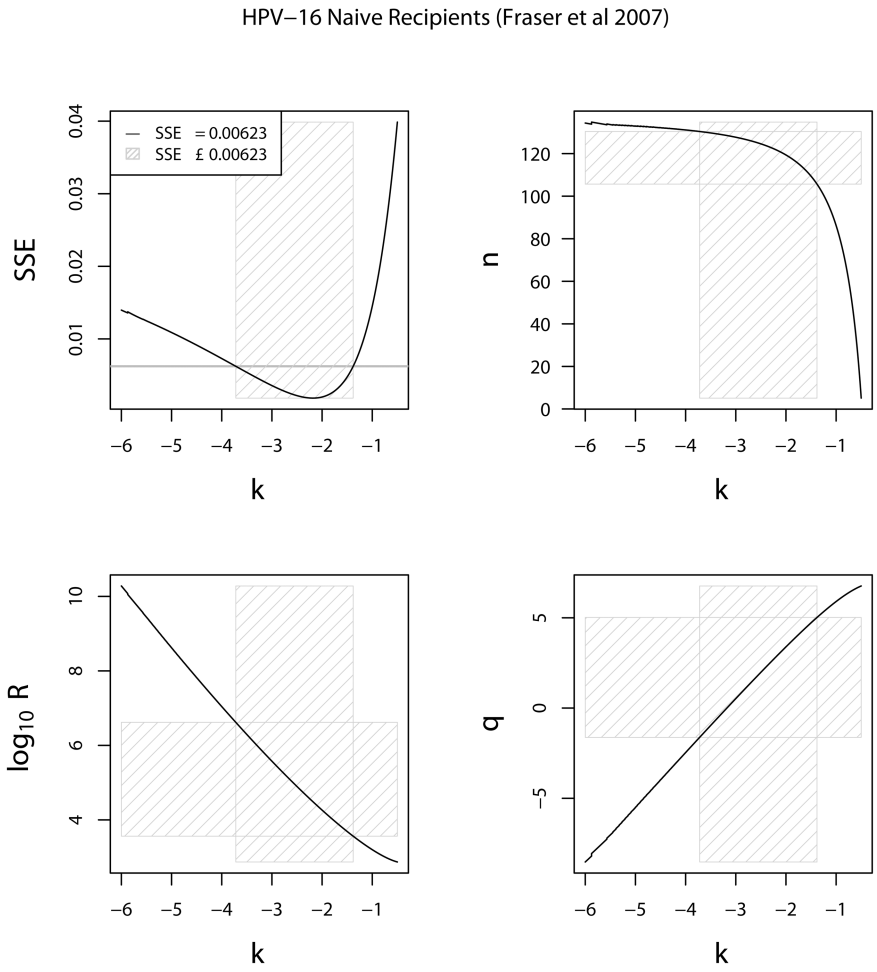

Figure 2.

LS parameters for OPLD/MPLD obtained by varying power exponent parameter *k*. Fits are based on reported GMTs from ref. 12 (HPV-16 naive subjects). In top left plot the SSE (= 0.00623) attained using OPLD/MPLD parameters reported in ref. 12 is indicated by the horizontal gray line. Regions of the parameter space associated with SSE ≤ 0.00623 are cross-hatched.

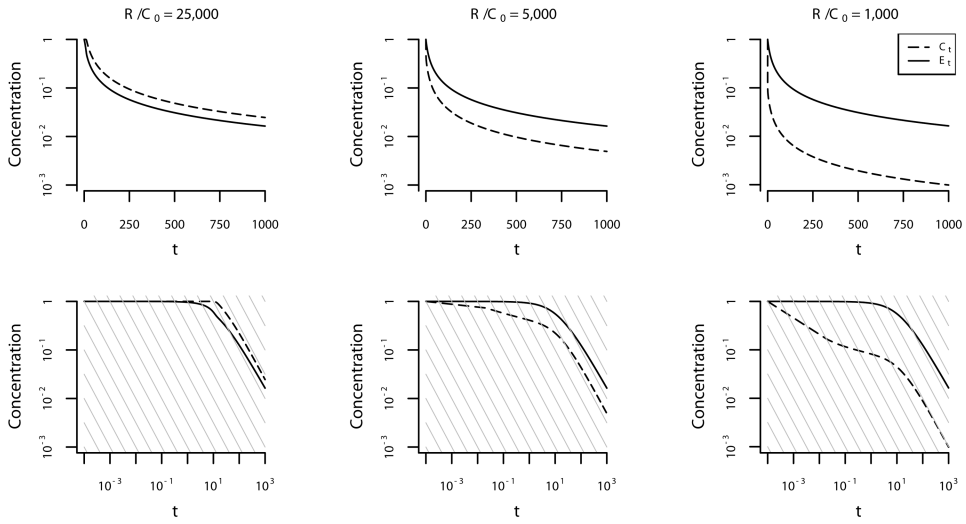

Figure 3.

Plots show model pathways for varying total resource R/C_0 = 25000, 5000, 1000 (columns 1-3). In row 1 plots of C_t and E_t are shown with a vertical log-scale. Row 2 shows C_t and E_t on a log-log scale. Grid lines parallel to t^{-1} are superimposed. For display purposes E_0, C_0 are both normalized to equal 100% in rows 1-2.

Table 1

Classification of four models: *power-law decay* (PLD); *reciprocal-time decay* (RTD); *offset power-law decay* (OPLD); *offset reciprocal-time decay* (ORTD). Equivalence to models defined in ref. 12 is indicated, in particular *conventional power-law decay* (CPLD); *modified power-law decay* (MPLD). All models conform to Equation (2) and are distinguished by various parametric constraints.

		Reciprocal-time decay:	
		Yes ($k = 0$)	**No ($k \geq 0$)**
Nonzero asymptote:	Yes ($v \geq 0$)	ORTD	OPLD [= MPLD[12]]
	No ($v = 0$)	RTD	PLD [= CPLD[12]]

Table 2

List of studies used in review of post-vaccination antibody kinetics.

Vaccine Type	Study
Review 1 - Model PLD	
Hepatitis-B	Gesemann & Scheiermann (1995)[15]
Hepatitis-B	Honorati et al (1999)[16]
Haemophilus influenzae type b	Southern et al (2007)[17]
Meningococcal serogroup C and *haemophilus Influenzae* type b	Southern et al (2007);[17] Borrow et al (2010)[18]
Diptheria	Swart et al (2016)[19]
Review 2 - Models PLD, OPLD, RTD, ORTD	
HPV-16	Fraser et al (2007)[12]
Hepatitis-A	Wiedermann et al (1997)[20]
Acellular pertussis	Le et al (2004)[21]